

Role of Spacer Chain Length in Dimeric Micellar Organization. Small Angle Neutron Scattering and Fluorescence Studies

Soma De,[†] Vinod K. Aswal,[‡] Prem S. Goyal,[‡] and Santanu Bhattacharya*[†]

Department of Organic Chemistry, Indian Institute of Science, Bangalore 560 012, India; and Solid State Physics Division, Bhabha Atomic Research Centre, Bombay 400 085, India

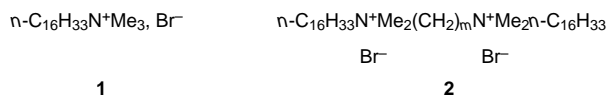
Received: November 30, 1995; In Final Form: March 4, 1996[⊗]

Micelles of different dimeric amphiphiles Br^- , $n\text{-C}_{16}\text{H}_{33}\text{NMe}_2^+-(\text{CH}_2)_m-\text{N}^+\text{Me}_2-n\text{-C}_{16}\text{H}_{33}$, Br^- (where $m = 3, 4, 5, 6, 8, 10,$ and 12) adopt different morphologies and internal packing arrangements in aqueous media depending on their spacer chain length (m). Detailed measurements of small angle neutron scattering (SANS) cross sections from different bis-cationic, dimeric surfactant micelles in aqueous media (D_2O) are reported. The data have been analyzed using the Hayter and Penfold model for macro ion solution to compute the interparticle structure factor $S(Q)$ taking into account the screened Coulomb interactions between the dimeric micelles. The SANS analysis clearly indicated that the extent of aggregate growth and the variations of shapes of the dimeric micelles depend primarily on the spacer chain length. With spacer chain length, $m \leq 4$, the propensity of micellar growth was particularly pronounced. The effects of the variation of the concentration of dimeric surfactants with $m = 5$ and 10 on the SANS spectra and the effects of the temperature variation for the micellar system with $m = 10$ were also examined. The critical micelle concentrations (cmc) and their microenvironmental feature, namely, the microviscosities that the dimeric micellar aggregates offer to a solubilized, extrinsic fluorescence probe, 1,6-diphenyl-1,3,5-hexatriene, were also determined. The changes of cmcs and microviscosities as a function of spacer chain length have been explained in terms of conformational variations and progressive looping of the spacer in micellar core upon increasing m values.

Introduction

Surfactant molecules, which contain a polar headgroup and hydrophobic chain, are capable of producing supramolecular assemblies that possess properties distinctly different from those of the individual monomeric molecules prior to aggregation.^{1a,b} As a matter of fact, a whole variety of aggregate morphologies, e.g., micelles, bilayers, lamellae, and vesicles, have all been observed.² Correlation of molecular architecture of different surfactants with the aggregate morphologies they produce upon self-assembly is important because understanding polymorphism at the molecular level helps to develop materials that find utility in household and industrial applications.³

Generally, micelles are formed upon dispersion of *single-chain* surfactants in water, e.g., **1**, cetyltrimethylammonium bromide (CTAB). Recently, a new class of surfactant has been introduced.⁴ These surfactants, in contrast to their more traditional (single-chain/single polar headgroup) counterparts, are made of two hydrophobic chains and two hydrophilic headgroups covalently attached through a spacer, e.g., **2**. Such



dimeric surfactants are also known as gemini and a few of them possess exceptional properties, such as a very low critical micellar concentration, high viscoelasticity, and an enhanced propensity for lowering the oil–water interfacial tension in comparison to their single-chain analogues.⁵ Consequently,

geminis are putative candidates for the next generation of surfactants⁶ and attracting a lot of current interest.

Upon dispersion in water, hydrocarbon segments in a surfactant tend to minimize water exposure and thus prefer to self-aggregate and organize closely. The force that drives this aggregation is entropic in origin and facilitates the release of “structured” water molecules.⁷ But while the hydrocarbon chains pack closer to minimize water contacts, the polar headgroups of identical charge tend to stay away from each other as a result of electrostatic repulsion and extensive headgroup hydration. In a micellar aggregate, thus an “equilibrium” distance between the polar heads is maintained as a result of compromise between the two opposing tendencies. Since the polar headgroups are *covalently connected* by a linkage within a gemini surfactant itself, the separation between the polar headgroups within a dimeric unit depends both on the nature (rigid vs flexible) and the length of the spacer.⁸ Thus, when the spacer is *flexible*, e.g., a polymethylene chain $(\text{CH}_2)_m$, and the length of the spacer is *shorter* ($m \leq 4$) than the equilibrium separation between the two polar headgroup charges, the spacer chain will tend to remain in as much extended conformation as possible to minimize the electrostatic repulsion. However, this conformational arrangement arises only at the expense of “undesirable” contacts of the hydrocarbon spacer with bulk water. On the contrary, when the spacer chain length is *longer* than this equilibrium distance between the charged polar headgroups, the spacer chain will tend to loop into the micelle interior in order to avoid its exposure to water.

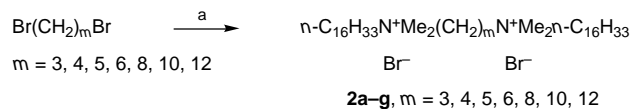
Micelles and other related organized assemblies of relatively well-known surfactant structures have been the subject of intense research for a number of years. Attempts have been directed toward the elucidation of micellar structures for numerous surfactants under a variety of experimental conditions. Due to our interest in the aggregate chemistry we had earlier examined micelles,⁹ vesicles,¹⁰ and other supramolecular aggregates.¹¹

* To whom correspondence should be addressed. Fax: 91-080-334-1683. E-mail: sb@pople.orgchem.iisc.ernet.in.

[†] Indian Institute of Science.

[‡] Bhabha Atomic Research Centre.

[⊗] Abstract published in *Advance ACS Abstracts*, May 1, 1996.

SCHEME 1: a: C₁₆H₃₃NMe₂ (3.0 equiv), Dry EtOH, Reflux, 48 h; 70–90% Yield

Although there is lot of current interest in the dimeric micellar system, much less is known about their micelle structure at ambient temperatures. Different surfactant systems have been earlier examined by neutron scattering.^{12–14} Neutron scattering has been extensively used also for the examination of different membrane structures.¹⁵ Recently, a report describing the small angle neutron scattering spectra of a different dimeric surfactant system, 10-*m*-10,2Br[−], i.e., [C₁₀H₂₁N⁺Me₂-(CH₂)_{*m*}N⁺Me₂C₁₀H₂₁, 2Br[−]] has appeared in the literature.¹⁶ The present work describes SANS spectra of dimeric micelles composed of 16-*m*-16,2Br[−] surfactants **2**, where, *m* = 3, 4, 5, 6, 8, 10, and 12. This chain length is equal to that present in the well-known monomeric cationic surfactant, cetyltrimethylammonium bromide (**1**). Since the details of the micellar properties of **1** is well documented in literature, the present study allows us to compare these results directly with that of **1**. To understand the role of flexible spacer chain such as length and to gain adequate insight into their role in determining the microstructures of dimeric surfactant micelles, we have performed SANS experiments employing gemini micelles of different spacer chain length. The effect on SANS spectra upon variation of concentration with dimeric surfactant of specific *m* value and the effect of temperatures on the neutron cross sections was also examined. To combine the information available from SANS studies with other micellar properties, the effects of *m* values on the critical micellar concentrations and microviscosities were also studied with 16-*m*-16,2Br[−] surfactants, **2**.

Experimental Section

General Methods. Cetyltrimethylammonium bromide (CTAB), *n*-hexadecyl bromide, and α,ω -dibromoalkanes were purchased from Aldrich Chemical Co. *N,N*-Hexadecyl-*N,N*-dimethylamine was obtained by refluxing *n*-hexadecyl bromide with dimethylamine (Merck, 40% solution in water) in dry ethanol at 80 °C for 24 h. ¹H NMR spectra were recorded in Bruker SEM-200 (200 MHz) NMR spectrometer. Chemical shifts (δ) are reported in ppm downfield from the internal standard. Microanalyses were performed on a Carlo Erba elemental analyzer Model 1106. All the reagents and solvents were highest grade available commercially and used purified, dried or freshly distilled as required. Steam-distilled water was used for all physical measurements.

Dimeric Surfactants. The dimeric surfactants were synthesized as indicated in the following (Scheme 1).

Synthesis of Bis(quaternary ammonium) Surfactants (2a–2g). The bis(quaternary ammonium) surfactants **2a–2g** were synthesized as described in detail in the following.

All the surfactants **2a–2g** were obtained by refluxing the corresponding α,ω -dibromoalkanes (*m* = 3, 4, 5, 6, 8, 10, and 12) with *N,N*-hexadecyl-*N,N*-dimethylamine in dry ethanol (at ~80 °C) for 48 h. The solvent was removed under vacuum from the reaction mixture and the solids thus obtained were recrystallized from hexane/ethyl acetate mixture for at least three times to obtain pure compounds. The overall yields of the surfactants ranged from 70 to 90%. All the compounds were characterized adequately and gave satisfactory ¹H NMR and C,H,N analysis. Pertinent details are given below.

Bis(hexadecyldimethylammonium)propane (2a). ¹H NMR (200 MHz, CDCl₃) δ 0.87 (t, 6 H, alkyl chain 2 × 1 CH₃),

1.24–1.40 (br m, 52 H, alkyl chain 2 × 13 CH₂), 1.75 (br s, 4 H, alkyl chain 2 × 1 CH₂CH₂N⁺), 2.64 (br s, 2 H, spacer chain 1 × 1 CH₂CH₂N⁺), 3.36 (s, 12 H, 2 × 2 N⁺CH₃), 3.46 (m, 4 H, alkyl chain 2 × 1 CH₂N⁺), 3.77 (m, 4 H, spacer chain 2 × 1 CH₂N⁺). C,H,N analysis, Calcd. for C₃₉H₈₄N₂Br₂·2.0H₂O: C 60.29, H 11.42, N 3.60. Found C 60.02, H 11.38, N 3.33.

Bis(hexadecyldimethylammonium)butane (2b). ¹H NMR (200 MHz, CDCl₃) δ 0.88 (t, 6 H, alkyl chain 2 × 1 CH₃), 1.25–1.40 (br m, 44 H, alkyl chain 2 × 11 CH₂), 1.70–2.00 (m, 12 H, alkyl chain 2 × 3 CH₂), 2.20 (br s, 4 H, spacer chain 1 × 2 CH₂CH₂N⁺), 3.30 (s, 12 H, 2 × 2 N⁺CH₃), 3.40–3.50 (m, 4 H, alkyl chain 2 × 1 CH₂N⁺), 4.00 (br s, 4 H, spacer chain 2 × 1 CH₂N⁺). C,H,N analysis, Calcd. for C₄₀H₈₆N₂Br₂·2.0H₂O: C 60.74, H 11.74, N 3.54. Found C 60.65, H 11.41, N 3.42.

Bis(hexadecyldimethylammonium)pentane (2c). ¹H NMR (200 MHz, CDCl₃) δ 0.88 (t, 6 H, alkyl chain 2 × 1 CH₃), 1.15–1.45 (br m, 42 H, alkyl chain 2 × 10 CH₂ and spacer chain 1 CH₂), 1.68 (crude t, 16 H, alkyl chain 2 × 4 CH₂), 2.02–2.20 (br m, 4 H, spacer chain 1 × 2 CH₂CH₂N⁺), 3.33 (s, 12 H, 2 × 2 N⁺CH₃), 3.45 (crude t, 4 H, alkyl chain 2 × 1 CH₂N⁺), 3.90 (crude t, 4 H, spacer chain 1 × 2 CH₂N⁺). C,H,N analysis, Calcd. for C₄₁H₈₈N₂Br₂: C 64.04, H 11.54, N 3.64. Found C 64.23, H 11.72, N 3.47.

Bis(hexadecyldimethylammonium)hexane (2d). ¹H NMR (200 MHz, CDCl₃) δ 0.88 (t, 6 H, alkyl chain 2 × 1 CH₃), 1.15–1.45 (s + br m, 48 H, alkyl chain 2 × 12 CH₂), 1.62 (br m, 12 H, spacer chain 1 × 2 CH₂CH₂N⁺ and alkyl chain 2 × 1 CH₂CH₂CH₂N⁺), 2.08 (br s, 4 H, spacer chain 1 × 2 CH₂CH₂CH₂N⁺), 3.38 (br s, 16 H, 2 × 2 N⁺CH₃ and alkyl chain 2 × 1 CH₂N⁺), 3.73–3.81 (m, 4 H, spacer chain 1 × 2 CH₂N⁺). C,H,N analysis, Calcd. for C₄₂H₉₀N₂Br₂: C 64.43, H 11.58, N 3.58. Found C 64.27, H 11.78, N 3.36.

Bis(hexadecyldimethylammonium)octane (2e). ¹H NMR (200 MHz, CDCl₃) δ 0.88 (t, 6 H, alkyl chain 2 × 1 CH₃), 1.25–1.90 (s + br m, 68 H, alkyl chain 2 × 14 CH₂ and spacer chain 1 × 6 CH₂), 3.36 (s, 12 H, 2 × 2 N⁺CH₃), 3.44–3.50 (m, 4 H, alkyl chain 2 × 1 CH₂N⁺), 3.71–3.76 (m, 4 H, spacer chain 1 × 2 CH₂N⁺). C,H,N analysis, Calcd. for C₄₄H₉₄N₂Br₂: C 65.16, H 11.68, N 3.45. Found C 65.05, H 11.88, N 3.20.

Bis(hexadecyldimethylammonium)decane (2f). ¹H NMR (200 MHz, CDCl₃) δ 0.88 (t, 6 H, alkyl chain 2 × 1 CH₃), 1.25–1.50 (s + br m, 64 H, alkyl chain 2 × 13 CH₂ and spacer chain 1 × 6 CH₂), 1.60 (br t, 8 H, spacer chain 1 × 2 CH₂CH₂N⁺, and alkyl chain 2 × 1 CH₂CH₂N⁺), 3.40 (s, 12 H, 2 × 2 N⁺CH₃), 3.46 (t, 4 H, alkyl chain 2 × 1 CH₂N⁺), 3.70–3.85 (m, 4 H, spacer chain 1 × 2 CH₂N⁺). C,H,N analysis, Calcd. for C₄₆H₉₈N₂Br₂·3.0H₂O: C 61.86, H 11.73, N 3.13. Found C 62.25, H 11.42, N 2.95.

Bis(hexadecyldimethylammonium)dodecane (2g). ¹H NMR (200 MHz, CDCl₃) δ 0.88 (t, 6H, alkyl chain 2 × 1 CH₃), 1.25–1.38 (s + br m, 68 H, alkyl chain 2 × 13 CH₂ and spacer chain 1 × 8 CH₂), 1.65–1.85 (br m, 8 H, spacer chain 1 × 2 CH₂CH₂N⁺ and alkyl chain 2 × 1 CH₂CH₂N⁺), 3.38 (s, 12 H, 2 × 2 N⁺CH₃), 3.44–3.54 (m, 4 H, alkyl chain 2 × 1 CH₂N⁺), 3.64–3.74 (m, 4 H, spacer chain 1 × 2 CH₂N⁺). C,H,N analysis, Calcd. for C₄₈H₁₀₂N₂Br₂·0.5H₂O: C 65.80, H 11.85, N 3.20. Found C 66.09, H 12.09, N 3.05.

Determination of Critical Micellar Concentrations (Cmc).

Fluorescence technique was used to determine the critical micellar concentrations. 1,6-Diphenyl-1,3,5-hexatriene (DPH, purchased from Aldrich Chemical Co.), a fluorescence probe whose emission quantum yield gets enhanced upon incorporation from water into a micelle,¹⁷ was chosen as the probe. Fluorescence measurements were done in a Hitachi F-4500 fluo-

rescence spectrophotometer equipped with a thermostated water-circulating bath (Julabo Model F10). All the measurements were carried out at 30 °C and using a 3 cm³ cell. Excitation wavelength was fixed at 360 nm and emission spectra of the region 390–480 nm were studied. Bandwidths were fixed at 5 nm for both the emission and excitation spectra. Surfactant solutions of different concentrations in water were doped with DPH for each amphiphile for cmc determination. Then the cmc was determined from the plot of the concentration of the surfactant vs the corresponding fluorescence intensity at 430 nm.

Determination of Microviscosities ($\bar{\eta}$). The fluorescence anisotropy (r) of DPH as sensed by micelle doped DPH was calculated from the intensities obtained at 0–0°, 0–90°, 90–0°, and 90–90° angle settings of the excitation and emission polarization accessories, respectively, and using an appropriate correction factor. Specifically, the temperature of the cuvette containing the sample was maintained at 30 °C or any other temperature by the use of a thermostated temperature controlling water-circulating bath (Julabo Model F10) for 10 min to allow for thermal equilibration. The fluorescence intensities of the emitted light polarized parallel (I_{\parallel}) and perpendicular (I_{\perp}) to the exciting light were recorded. These fluorescence intensities were corrected for scattered light intensity, which was determined independently for an unlabeled reference suspension by the same procedure. The fluorescence anisotropy (r) for each amphiphile at 30 °C was calculated according to $r = (I_{\parallel} - GI_{\perp}) / (I_{\parallel} + 2GI_{\perp})$, where G is the grating correction factor. Microviscosities ($\bar{\eta}$) of the micellar systems in which the fluorophore is placed were calculated using anisotropy values.¹⁷ The measurements were done at a fixed 50 mM concentration for **2a–2g** and at 100 mM concentration for CTAB.

Small Angle Neutron Scattering (SANS) Measurements

Data Collection. Small angle neutron scattering (SANS) experiments were carried out on 16-*m*-16,2Br[−] samples for $m = 3, 4, 5, 6, 8, 10,$ and 12 . All of the final solutions used in neutron-scattering experiments were prepared in D₂O. D₂O was obtained from Heavy Water Division of BARC and was at least 99.5 atom % D pure. This provides a very good contrast between the micelle and the solvent in a SANS experiment. Neutron-scattering measurements were performed on the 7.0 m (source-to-detector distance) SANS instrument at the CIRUS Reactor, Trombay. The sample-to-detector distance was 1.8 m for all runs. This spectrometer makes use of a BeO filtered beam and has a resolution ($\Delta Q/Q$) of about 15% and $Q = 0.05 \text{ \AA}^{-1}$. The angular distribution of the scattered neutrons is recorded using a one-dimensional position-sensitive detector (PSD). The accessible wave vector transfer, $Q (=4\pi \sin^{1/2}\phi/\lambda)$, where λ is the wavelength of the incident neutrons and ϕ is the scattering angle), range of this instrument is between 0.02 and 0.3 Å^{-1} . PSD allows a simultaneous recording of the data over the full Q range. The wavelength was $\lambda = 0.52 \text{ nm}$.

The solutions were held in a 0.5 cm path length UV grade quartz sample holder with tight-fitting Teflon stoppers, sealed with parafilm. In most of the measurements, the surfactant concentration ($c = 50 \text{ mM}$) and the sample temperature ($30 \pm 0.1 \text{ °C}$) were maintained fixed. The effect of different concentration on the SANS distribution was studied for 16-5-16,2Br[−] and 16-10-16,2Br[−] micellar samples for concentration in the range of 25–100 mM. The effect of temperature was also investigated for the 16-10-16,2Br[−] micellar system at a fixed surfactant concentration of $c = 100 \text{ mM}$.

Data Treatment. Scattering intensities from the surfactant solutions were corrected for detector background and sensitivity,

empty cell scattering, and sample transmission. Solvent intensity was subtracted from that of the sample. The resulting corrected intensities were normalized to absolute cross section units and thus $d\Sigma/d\Omega$ vs Q was obtained. This absolute calibration has an estimated uncertainty of 10%. The experimental points are fitted using a nonlinear least-squares routine as described below. Comparisons between the experimental and the calculated cross sections are shown in Figures 1–4.

Analysis of SANS Data

1. Calculation of the Scattering Intensity. The coherent differential scattering cross section, $d\Sigma/d\Omega$, derived by Hayter and Penfold¹⁸ and Chen¹⁹ can be reduced to eq 1 for an assembly of *monodisperse*, uniform ellipsoidal micelles, where n denotes

$$d\Sigma/d\Omega = nV_m^2(\rho_m - \rho_s)^2P(Q)S(Q) \quad (1)$$

the number density of the micelles, ρ_m and ρ_s are respectively the scattering length densities of the micelle and the solvent, and V_m is the volume of the micelle. $P(Q)$ is the single (orientationally averaged) particle (intraparticle) structure factor and $S(Q)$ is the interparticle structure factor. The aggregation number N for the micelle is related to the micellar volume V_m by the relation $N = V_m/v$, where v is the volume of the individual surfactant molecule.

As the value of v for a gemini surfactant molecule is not known, we have rewritten the above equation in terms of v . Thus, the eq 1 can be rewritten as follows.

$$d\Sigma/d\Omega = cN(b_m - v\rho_s)^2P(Q)S(Q) \quad (2)$$

where $c (=nN)$ is the surfactant concentration and $b_m (= \rho_m v)$ is the total coherent scattering amplitude of the surfactant molecule.

The form factor $P(Q)$ for an ellipsoidal particle is given by eq 3, i.e.,

$$P(Q) = \int [F(Q,\mu)]^2 d\mu \quad (3)$$

The form factor, $F(Q,\mu)$ is given by eq 4, i.e.,

$$F(Q,\mu) = 3(\sin w - w \cos w)/w^3 \quad (4)$$

where $w = Q[a^2\mu^2 + b^2(1 - \mu^2)]^{1/2}$ and a and b are respectively the semiminor and semimajor axes of the ellipsoid of revolution. That is, $P(Q)$ depends on a and b .

2. Structure Factor for Interacting Micelles. The interparticle structure factor $S(Q)$ depends on the spatial distribution of micelles. In the following analysis, we calculate $S(Q)$ using rescaled mean spherical approximation as developed by Hansen and Hayter.^{18c} This theory is applicable if there is no angular correlation between the particles. This assumption is quite reasonable for *charged* micelles especially when the surfactant concentration is small and if the ratio of the axes is not much greater than unity. Strong electrostatic repulsions prohibit close proximity of two micelles. The ellipsoidal micelle is approximated by an equivalent sphere of radius $R = (a^2b)^{1/3}$, the intermicellar interaction is modeled via a screened Coulomb potential and $S(Q)$ is calculated in mean spherical approximation. In this analysis, the only unknown parameter in $S(Q)$ is the effective monomer charge, α .

The data in Figure 1 (corresponding to different $m = 4, 5, 6, 8, 10,$ and 12) were first analyzed in terms of eq 2. $N, v, a,$ and α were taken as the parameters of the fit. The solid lines in Figure 1 are the calculated curves. The major axis $b (3Nv/4\pi a^2)$ was obtained from a knowledge of the above parameters.

TABLE 1: Effect of Spacer Length (m) in 16- m -16,2Br⁻ Micellar Systems on Q Value^a

space length m	aggregation no. N	effective monomer charge α	monomer vol. v (\AA^3)	semiminor axis $a = c$ (\AA)	semimajor axis b (\AA)	b/a
0	160	0.098	595	22.3	45.7	2.05
3				26.0	88.5	3.40
4				24.0	92.1	3.84
5	138	0.102	1500	22.0	102.2	4.65
6	97	0.106	1320	21.5	66.2	3.08
8	43	0.320	1850	20.3	45.7	2.25
10	50	0.247	1660	20.1	49.2	2.44
12	53	0.238	1880	18.9	66.1	3.50

^a All the SANS spectra were taken at 30 °C using 50 mM 16- m -16,2Br⁻ micelles. ^b 16- m -16,2Br⁻ molecules may be considered as the dimer of two CTAB monomers linked by a (CH₂) _{m} spacer. For CTAB, m is assumed to be zero and the SANS data were collected with 100 mM CTAB.

The values of N , α , a , b , and v are given in Table 1. The effects of concentration and temperature on size parameters for $m = 10$ and 5 were also obtained by similar methods. However, in these cases the values of a and v were kept fixed at the values, which were obtained from $c = 50$ mM and $T = 30$ °C data.

Results and Discussion

In a neutron scattering experiment, a beam of neutrons is directed upon the sample under examination and the intensities of the neutron scattering in different directions are measured. Since neutrons are scattered by the nuclei in the sample, even isotopes of the same elements can differ in their scattering power. Thus, by taking aggregates in D₂O rather than in H₂O, the scattering densities of various regions can be obtained, since deuterons and protons differ widely in their respective scattering capacities. As reported earlier,^{12–16} SANS measurements provide useful information pertaining to the shapes of various self-organizing systems in a noninvasive manner. Consequently, we examined how a specific series of dimeric micelles adopt different morphologies and internal packing arrangements in aqueous media depending on their spacer chain length (m) using the SANS experiments.

First, we report the results of the measurements of neutron cross sections from the micellar solutions of dimeric surfactants 16- m -16,2Br⁻ in D₂O as a function of m values at a fixed surfactant concentration (50 mM). Measurements have covered Q ranges from 0.02 to 0.16 \AA^{-1} . For the sake of comparison, the data for pure CTAB solution ($c = 100$ mM, a concentration at which CTAB is known to form elongated, nonspherical micelles²⁰) are also shown in Figure 1. SANS distributions for 50 mM 16- m -16,2Br⁻, $m = 5, 6, 8, 10,$ and 12, show well-defined peaks as is the case with pure 100 mM CTAB solution. This peak arises because of a corresponding peak in the interparticle structure factor $S(Q)$. Usually, this peak occurs at $Q_m \sim 2\pi/d$, where d is the average distance between the micelles. Since the Q_m was found to vary with m , one can easily conclude that the number density (n) of micelles is not the same in above samples even when they have identical surfactant concentration. The $m = 3$ and 4 samples do not show the correlation peak suggesting that for these dispersions $Q_m < 0.02$ \AA^{-1} . The above observations further imply that the aggregation number of the micelle, N , depends on the spacer chain length m . It is not, however, apparent that the micelles are spherical. Consequently, in the following analysis, we assume them to be prolate ellipsoids ($a = c \neq b$), sphere being a special case of that.

Notably, the above method of data analysis did not give meaningful parameters for $m = 3$ data in Figure 1. This was

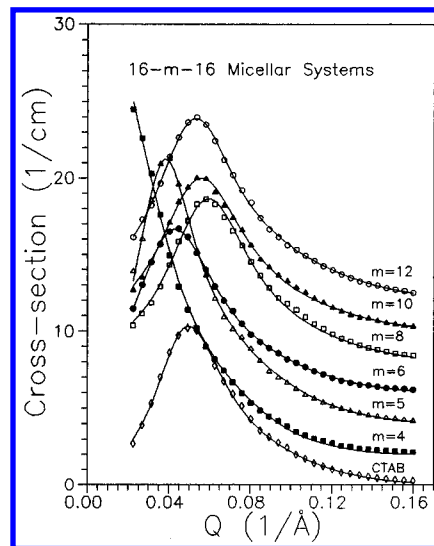


Figure 1. SANS distributions from different 16- m -16,2Br⁻ dimeric micellar systems at specified concentration (50 mM) at 30 °C. The lines shown are theoretical fits and the solid marks are experimentally determined data points.

partly because of the fact that the data for these samples did not show any correlation peak that occurred at a Q value which was lower than that examined in the present studies. In view of the above, these data were analyzed assuming $S(Q) = 1$.

Solubilization of 16- m -16,2Br⁻ surfactants at 50 mM concentration in pure D₂O required heating for $m = 3–5$. But the surfactants with m values > 5 could be readily dissolved in D₂O. Once solubilized, the dispersions were optically translucent and were stable for 5–6 h for $m = 3$ and 4, for 2–3 days for $m = 5$ and 6 and for several weeks for $m > 6$. Therefore, all the data presented herein used freshly prepared solutions. But the resulting solutions for $m = 3$ and 4 were found to be extremely viscous and this caused practical difficulties in their preparation and satisfactory experimental examination of micellar dispersions at this concentration. Both of these samples did not give any peak corresponding to the range of Q values that one could examine in this equipment. Such behavior is suggestive of pronounced ellipsoidal character (formation of threadlike aggregates) at 50 mM concentration for $m = 3$ or 4. Lower Q values also indicate that the number of micelles per unit volume is smaller for $m = 3$ or 4. Generally, the neutron scattering data obtained with the 16- m -16,2Br⁻ samples with $m = 3$ or 4 appeared to depend also on the thermal history of the sample suggesting aggregate growth upon aging. These findings are consistent with the earlier observation by Zana and co-workers^{5,20} with dimeric surfactants with short spacers having a very strong propensity for micellar growth and formation of micelles of very low curvature.

At a fixed concentration (50 mM) of the dimeric surfactants, 16- m -16,2Br⁻ in D₂O, the aggregation number, N , appeared to increase with the decrease in spacer chain length (decreasing m value). Reliable estimates of aggregation number could not be obtained for dimeric micelles with $m = 3$ and 4. The effective fractional charge (α) on micelles increased with increasing spacer chain length although not monotonically. Since spheroids and ellipsoids differ in terms of curvature, larger effective charge would be expected for a spheroidal micelle and smaller effective charge would be indicated for an ellipsoidal morphology. α showed a maximum at $m = 8$ and N showed a minimum at the same m value. Thus, it appears that for dimeric 16- m -16,2Br⁻ micelles with m values 8, 10, and 12, the shape of the micelles progressively becomes less elliptical (more spherical) at 50 mM concentration. On the other

hand, substantially lower α values for micelles with $m = 5$ and 6 indicate more ellipsoidal morphology. This is further substantiated by the changes in b/a values as a function of spacer chain length (Table 1). Within the dimeric surfactants with *even* m values, b/a values tend to decrease as m values increase from 4 to 8 and then increase again as m values goes from 8 to 12. The higher value of b/a for $m = 5$ could be a consequence of altered chain arrangement with odd m value in contrast to their counterparts with spacer chain having even number of methylene groups.

The experimentally determined values (SANS) for monomer volume (v) as defined earlier show a nonmonotonous behavior in terms of the variation with m value. An initial increase of v at $m = 8$ was seen and then the monomer volume maximizes at $m = 12$ at fixed 50 mM concentration for 16- m -16,2Br⁻ micelles. One outcome of covalent spacer insertion between two dimethylammonium ions at the level of headgroups is the imposition of additional geometric constraints on the surfactant intramolecular packing. This in turn influences the aggregate morphology. The packing parameter (p), introduced by Israelachvili et al.,²¹ is related with aggregate morphology in aqueous solutions at a concentration higher than the critical micellar concentration (cmc) by the equation $p = v/la$, where v is the volume occupied by the hydrophobic moiety of the surfactant molecule, l is the critical length in the fully extended conformation, and a is the surface area occupied by a surfactant headgroup at the water/micelle hydrophobic core interface. Both l and v can be calculated using Tanford's equations.²² As long as the hydrophobic tail length is constant, l is likely to remain the same amongst all 16- m -16,2Br⁻ derivatives and v is expected to increase *monotonically* with increase in m value. But as reported by Zana and co-workers with 12- m -12,2Br⁻ systems,²³ a was found to change with m in a *nonmonotonic* fashion. In particular, they found that a increases abruptly for $m = 3-8$ and following a maximum for $m = 10-12$ and then decreasing with $m > 12$. This experimental finding was also recently supported independently by Andelman and co-workers through a theoretical model.²⁴ In view of the above, we believe that among the 16- m -16,2Br⁻ systems which have been examined herein, micelles having a spacer chain with $m = 8$ might approach a maximum surface area occupied by its surfactant headgroups at the water/micelle hydrophobic core interface. This could explain why for $m = 8$ the Q value is higher than for the micelles that have m values > 8 .

Estimation of Equilibrium Separation between the Two Polar Head Groups within a Dimeric Surfactant. In aqueous solutions, at high concentrations, the two positively charged head groups within a dimeric surfactant unit will try to maintain a critical distance between them to minimize the Coulombic repulsion. But since such situation will create unfavorable water contacts with hydrophobic spacer chain, a separation equilibrating these two opposing tendencies will result. This has prompted us to estimate this critical distance based on our SANS data, assuming it to be equal to $\sqrt{4\pi a_{\text{eff}}^2/N}$, where $a_{\text{eff}} = (a^2b)^{1/3}$, considering the micelles to be *ellipsoidal*. Applying this, we have obtained a value of 7.94 Å for CTAB ($m = 0$) which is in reasonable agreement with the estimated value as reported by Zana et al.⁵ The same way, we calculated the critical distances between the two cationic centers for 2c-2g which came out to be 11.1, 11.0, 14.4, 13.6, and 14.0 Å, respectively.

Effect of Surfactant Concentration Variation. The effects of surfactant concentration on SANS distributions are shown in Figures 2 and 3 at 30 °C. As already indicated, the peak in $d\Sigma/d\Omega$ arises from intermicellar interference effects and occurs at $Q_m = 2\pi/d$, where d is average distance between the micelles.

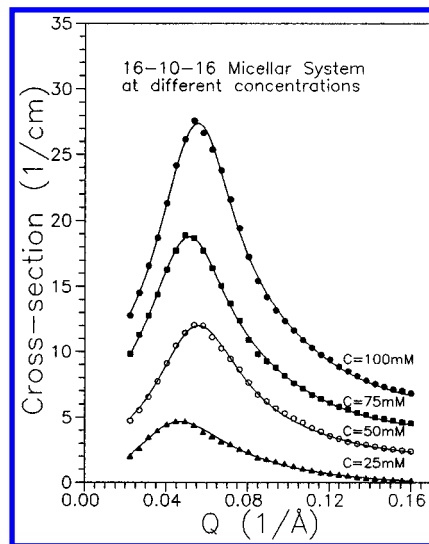


Figure 2. SANS distributions from 16-10-16,2Br⁻ dimeric micelles at different concentrations: 25 mM (▲), 50 mM (○), 75 mM (■), and 100 mM (●) at 30 °C.

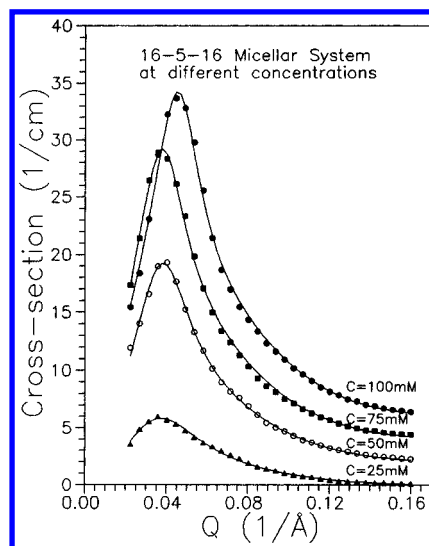


Figure 3. SANS distributions from 16-5-16,2Br⁻ dimeric micelles at different concentrations: 25 mM (▲), 50 mM (○), 75 mM (■), and 100 mM (●) at 30 °C.

With an increase in concentration, the interparticle distance decreases and the peak shifts to lower Q values. We examined the effect of concentration variation with two different micellar systems, one with spacer chain having *even* number of CH₂ groups, i.e., $m = 10$, and other with a spacer chain with *odd* number of CH₂ groups, i.e., $m = 5$.

Figure 2 shows the effect of concentration variation of 16-10-16,2Br⁻ at 30 °C. The concentration range examined was from 25 to 100 mM. The volume of one surfactant molecule in the micelle was taken to be independent of concentration of 16-10-16,2Br⁻. The monomer volume (v) for 16-10-16,2Br⁻ was found to be about 1660 Å³. It is seen that the calculated distributions give the peak positions in $d\Sigma/d\Omega$ with a good correspondence with experimentally determined points. As the concentration of 16-10-16,2Br⁻ is decreased, it is found that the peak in the measured distribution broadens with significant shifts in the peak position. The micellar shape changes from $b/a \sim 2.3$ to $b/a \sim 3.9$ (more oblate ellipsoidal) upon increase in concentration of 16-10-16,2Br⁻ from 25 to 75 mM (Table 2). There is a small decrease in the b/a value upon further increase in the concentration of 16-10-16,2Br⁻. The aggregation number N does not vary from 25 to 50 mM, but it increases

TABLE 2: Effect of Concentration on Q Value, Studied for the Surfactant System 16-10-16,2Br⁻ at 30 °C

concn (mM)	aggregation no. N	effective monomer charge α	monomer ^a vol v (Å ³)	semiminor ^a axis $a = c$ (Å)	semimajor axis b (Å)	b/a
25	47	0.215	1660	20.1	45.9	2.28
50	50	0.247	1660	20.1	49.2	2.45
75	80	0.160	1660	20.1	78.6	3.91
100	87	0.180	1660	20.1	85.1	3.80

^a v and a were kept fixed in the fitting procedures.

TABLE 3: Effect of Concentration on Q Value, Studied for the Surfactant System 16-5-16,2Br⁻ at 30 °C

concn (mM)	aggregation no. N	effective monomer charge α	monomer ^a vol v (Å ³)	semiminor ^a axis $a = c$ (Å)	semimajor axis b (Å)	b/a
25	84	0.114	1500	22.0	62.0	2.82
50	138	0.102	1500	22.0	102.2	4.65
75	206	0.105	1500	22.0	152.2	6.92
100	174	0.157	1500	22.0	128.8	5.86

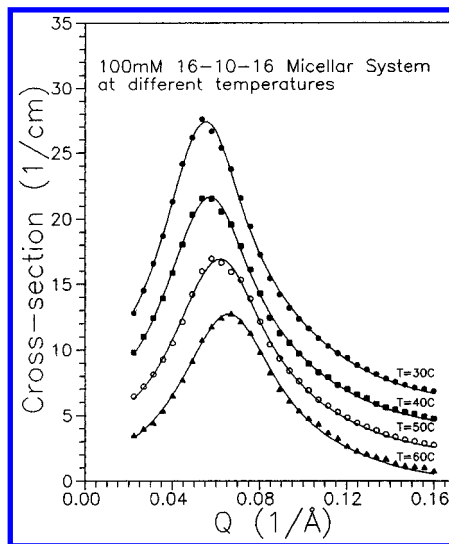
^a v and a were kept fixed in the fitting procedures.

appreciably with concentration > 50 mM. So, increase in Q_m value upon increase in concentration from 25 to 50 mM indicates an increase in number density of 16-10-16,2Br⁻ micelles. The tendency is, however, arrested upon further increase in concentration, and changeover of concentration > 50 mM results in the decrease in Q_m value, indicating sphere to ellipsoid morphological switchover. Increasing N for a given spacer chain length results in an increase in the axial ratio (b/a); i.e., as N increases, micellar shape tends to become more oblate elliptical. Since the shape of the micelle changes with respect to concentration, the interactions among charged headgroup of the dimeric 16-10-16,2Br⁻ units and water in the Stern layer region of the micelle appear to play an important role in determining the micellar shape. The effective fractional charge on the dimeric units of 16-10-16,2Br⁻ does change with concentration. However, this change is not regular.

Figure 3 shows the effect of concentration variation of 16-5-16,2Br⁻ at 30 °C. The concentration range examined was from 25 to 100 mM. Volume of one 16-5-16,2Br⁻ molecule in the micelle was again assumed to be independent of surfactant concentration. The monomer volume (v) for 16-5-16,2Br⁻ was found to be about 1500 Å³. It is again evident that the calculated distributions give the peak positions in $d\Sigma/d\Omega$ with a good correspondence with experimentally determined points. With 16-5-16,2Br⁻ micellar system, the micellar shape changes from b/a value of ~ 2.8 to ~ 6.9 (Table 3) as concentration rises from 25 to 75 mM probably due to onset of threadlike micellar shape at higher concentration.

With both 16-5-16,2Br⁻ and 16-10-16,2Br⁻ micelles, b/a values increase, although not monotonically with concentration showing a maximum around 75 mM concentration (Tables 2 and 3). The changes in the aggregation number, N , with both 16-5-16,2Br⁻ and 16-10-16,2Br⁻ micelles, follow similar trend with increase in concentration, showing a maximum around 75 mM. Effective surfactant charge (α) changes with respect to either the concentration or the spacer chain length. Changes in the effective surfactant charge with respect to the concentration with 16-5-16,2Br⁻ micellar systems appear to be more complex than the same for 16-10-16,2Br⁻ micelles. We believe that with 16-5-16,2Br⁻, more pronounced ellipsoidal character even at 50 mM concentration is responsible for its low α value.

Effect of Temperature. While for conventional single-chain surfactant micelles considerable information is available as to how micellar size varies with temperature, very little is known in this regard for gemini micelles. Zana et al. examined^{4b} the

**Figure 4.** SANS distributions from 100 mM 16-10-16,2Br⁻ dimeric micelles at various temperatures: 30 °C (●), 40 °C (■), 50 °C (○), and 60 °C (▲).**TABLE 4: Effect of Temperature on Q Value, Studied for the Surfactant System 16-10-16,2Br^{-a}**

temp (°C)	aggregation no. N	effective monomer charge α	monomer vol v (Å ³)	semiminor axis a (Å)	semimajor axis b (Å)	b/a
30	87	0.18	1660	20.1	85.1	4.23
40	77	0.18	1660	20.1	76.0	3.78
50	63	0.22	1660	20.1	62.2	3.10
60	54	0.25	1660	20.1	52.8	2.63

^a All the SANS spectra were taken using 100 mM 16-10-16,2Br⁻ micelles.

effect of temperature on the ionization (α) of the 12-3-12,2Br⁻ surfactant micelles and reported that α increases with temperature. Figure 4 shows the variation of neutron cross sections for 16-10-16,2Br⁻ micelles as the temperature is increased. The neutron cross sections build up at higher Q values as the temperature is increased. The peak in the measured distribution also broadens with the increase in temperature.

Table 4 records the information based on the above experimental findings as a function of temperature. Increase in temperature enhances the degree of ionization and in this way effects a modification of the magnitude of electrostatic repulsion. This results in a decrease in the aggregation number, N , upon increase in temperature. The effective fractional charge per monomer, however, appears to increase with increase in temperature. Since a smaller effective charge indicates a more ellipsoidal morphology, increasing temperature appears to induce ellipsoid to sphere transition for 16-10-16,2Br⁻. This notion is also supported by the concomitant decrease in b/a values upon increase in temperature.

Spacer Chain Length and Critical Micellar Concentrations. The cmc data for 16- m -16,2Br⁻ series have been summarized in Table 5. Figure 5 shows that cmc goes through a maximum around $m = 6$ and then decreases with further increase in m value. Similar lowering of cmc values was observed with both single chain (conventional) surfactants and bolophilic surfactants²⁵ when the hydrophobic chain length is enhanced. Zana and co-workers^{4b} independently examined the cmc data for 16- m -16,2Br⁻ surfactants by measuring their electrical conductivities of the resulting surfactant dispersions. Importantly, the cmc values obtained in this study from fluorescence probing (DPH) and the cmc values reported by Zana et al. using solution conductivities appear to be in good agreement. Strikingly, a maximum of cmc at $m = 6$ value for

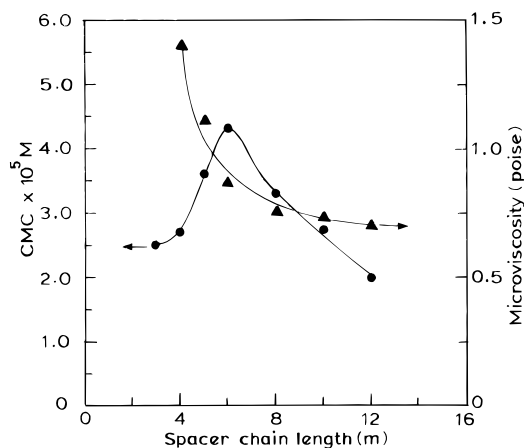


Figure 5. Variations of the critical micellar concentrations (●) and microviscosities (▲) of 16-*m*-16,2Br⁻ surfactants with the spacer chain length (*m*) at 30 °C.

TABLE 5: Dependence of Critical Micellar Concentrations and Microviscosities^a of 16-*m*-16,2Br⁻ Dimeric Micelles on Spacer Chain Length (*m*) at 30 °C

spacer length (<i>m</i>)	cmc × 10 ⁵ (M)	microviscosity ($\bar{\eta}$) ^a (P)
3	2.5 ± 0.15	1.445 ^b
4	2.7 ± 0.10	1.394
5	3.6 ± 0.10	1.102
6	4.3 ± 0.20	0.866
8	3.3 ± 0.15	0.752
10	2.7 ± 0.15	0.730
12	2.0 ± 0.10	0.704

^a Measured at 50 mM concentration for 16-*m*-16,2Br⁻ dimeric micelles at 30 °C. ^b At 45 °C $\bar{\eta}$ was determined. The sample in the cuvette turned highly turbid at 30 °C.

the same series of surfactants was also observed by Zana and co-workers. The changes in the cmc values could be a consequence of conformational changes of the spacer polymethylene chain within the dimeric surfactant ion and of gradual looping of a significant portion of the spacer polymethylene segment into the micellar interior. When a cis conformation of the surfactant monomer is adopted, it may result in establishment of some “contacts” between the hydrophobic tails. This could make the free energy of transfer for an amphiphile from the aqueous pseudophase to the aggregated state slightly less negative. This could cause the cmc to be higher for dimeric systems with low *m* values. At higher *m* values, the cmc appears to decrease which was also observed for *n*-C₁₂H₂₅NMe₂⁺(C₃H₇),Br⁻ micelles by Zana and co-workers.²⁶ A combination of the two above-mentioned factors could explain the maximal cmc value for 16-6-16,2Br⁻.

Dependence of Microviscosity ($\bar{\eta}$) on Spacer Chain Length.

Another parameter of considerable interest is the microenvironmental viscosity (microviscosity, $\bar{\eta}$) of the dimeric micellar aggregates. This parameter can be conveniently estimated by the determination of the fluorescence polarization of the probe, 1,6-diphenyl-1,3,5-hexatriene (DPH).¹⁷ Table 5 summarizes the microviscosity estimates of 16-*m*-16,2Br⁻ micelles at a fixed concentration of 50 mM as a function of variable *m* values. DPH is a fluorescence probe whose emission quantum yield gets enhanced upon partitioning into a micelle or a bilayer from water. Furthermore, the fluorescence polarization (*P*) or the anisotropy (*r*) of DPH allows us to estimate the microviscosity ($\bar{\eta}$) of the medium in which DPH is solubilized. The microviscosity we have measured agree for CTAB (100 mM) with that reported using DPH and other probes, around 0.56 P for CTAB.^{27,28} The microviscosities estimated herein show a very

clear trend. In other words, with the increase in *m* values, the microviscosities fall off. At a 25 mM concentration, CTAB micelles are spherical and give a microviscosity of approximately 0.55 P due to DPH incorporated in it. Addition of NaBr to the same CTAB micellar solution leads to the formation of rodlike micelles.²⁸ The resulting rodlike micelles gave a microviscosity estimate around 0.78 P due to DPH incorporated in it. Since sphere to rod transition in CTAB micelles upon addition of salt has been well documented, one may be tempted to infer that with decreasing microviscosities with increasing *m* values within dimeric micelles, the micellar morphology tends to be less ellipsoidal in shape. Such an inference is in agreement with the observed SANS data also.

Conclusions

Dimeric surfactants (16-*m*-16,2Br⁻ system) in which two quaternary ammonium centers are attached at the level of polar headgroup by a polymethylene spacer chain (CH₂)_{*m*}, *m* = 3–6, 8, 10, and 12, have been synthesized. For these dimeric surfactant micelles, the SANS spectra were measured and the cmc values were determined using an extrinsic fluorescence probe, DPH. From the detailed measurements of small angle neutron scattering cross sections, we have shown how dimeric micelles of the 16-*m*-16,2Br⁻ system change with *m* values. The morphological changes and micellar growth in different dimeric surfactant–water aggregates have been indicated. The aggregation number of such dimeric micelles was found to depend primarily on the spacer chain length. It has been found that an increase in the spacer chain length (*m* value) suppresses the tendencies of micellar growth of 16-*m*-16,2Br⁻ in water. Fluorescence studies also show strong dependence of parameters such as critical micellar concentrations and microviscosities on the spacer chain length (*m* value) in such system. Despite the fact that it describes a relatively complex situation, i.e., it takes into account the spacer chain looping and possible micellar growth particularly at higher concentrations, the presented scenario provides useful information pertaining to the shapes, concentration, and temperature dependence of the described dimeric surfactant family.

Acknowledgment. We thank the Department of Atomic Energy for financial support of this work (Grant BRNS/37/11/94-R&D-II/789). We also thank Dr. B. A. Dasannacharya for his encouragement and interest in this work.

References and Notes

- (1) (a) Wennerstrom, H.; Lindman, B. *Phys. Rep.* **1979**, *52*, 1. (b) Menger, F. M. *Angew. Chem., Int. Ed. Engl.* **1991**, *30*, 1086.
- (2) (a) Israelachvili, J. N. *Intermolecular and Surface Forces*, 2nd ed.; Academic Press: London, 1991. (b) Israelachvili, J. N. *Physics of Amphiphiles: Micelles, Vesicles and Microemulsions*; Elsevier: Amsterdam, 1985; p 24.
- (3) (a) Hoffmann, H.; Sturmer, A. *Tenside, Surfactants, Deterg.* **1993**, *30*, 335. (b) Cutler, W. G.; Vissa, E. *Detergency: Theory and Technology*; Marcel Dekker: New York, 1987. (c) Dobijs, B. In *Phenomena in Mixed Surfactant Systems*; Scamehorn, J. F., Ed.; ACS Symp. Ser.; American Chemical Society: Washington, DC, 1986; Vol. 311, p 216.
- (4) Menger, F. M.; Littau, C. A. *J. Am. Chem. Soc.* **1991**, *113*, 1451.
- (5) Zana, R.; Benraou, M.; Rueff, R. *Langmuir* **1991**, *7*, 1072.
- (6) Zana, R.; Talmon, Y. *Nature* **1993**, *362*, 228.
- (7) Rosen, M. J. *CHEMTECH* **1993**, *23*, 30.
- (8) Muller, N. *Acc. Chem. Res.* **1990**, *23*, 23.
- (9) Karaborni, S.; Esselink, K.; Hilbers, P. A. J.; Smit, B.; Karthaus, J.; van Os, N. M.; Zana, R. *Science* **1994**, *266*, 254.
- (10) Bhattacharya, S.; Snehaltha, K. *Langmuir* **1995**, *11*, 4653.
- (11) Bhattacharya, S.; De, S. J. *Chem. Soc., Chem. Commun.* **1995**, 651.
- (12) Bhattacharya, S.; Haldar, S. *Langmuir* **1995**, *11*, 4748. (c) Bhattacharya, S.; Subramanian, M.; Hiremath, U. *Chem. Phys. Lipids* **1995**, *78*, 177. (d) Moss, R. A.; Bhattacharya, S.; Chatterjee, S. *J. Am. Chem. Soc.* **1989**, *111*, 3623.

- (11) Ragunathan, K.; Bhattacharya, S. *Chem. Phys. Lipids* **1995**, *77*, 13.
- (12) (a) Berr, S. S.; Jones, R. R. M.; Johnson, J. S. *J. Phys. Chem.* **1992**, *96*, 5611. (b) Berr, S. S.; Jones, R. R. M. *Langmuir* **1988**, *4*, 1247.
- (13) (a) Pils, H.; Hoffmann, H.; Hoffmann, S.; Kalus, J.; Kencono, A. W.; Lindner, P.; Ulbricht, W. *J. Phys. Chem.* **1993**, *97*, 2745. (b) Chevalier, Y.; Zemb, T. *Rep. Prog. Phys.* **1990**, *53*, 279. (c) Kaler, E. W.; Billman, J. F.; Fulton, J. L.; Smith, R. D. *J. Phys. Chem.* **1991**, *95*, 458. (d) Prasad, D.; Singh, H. N.; Goyal, P. S.; Rao, K. S. *J. Colloid Interface Sci.* **1993**, *155*, 415. (e) Goyal, P. S.; Menon, S. V. G.; Dasannacharya, B. A.; Thiyagaragan, P. *Phys. Rev.* **1995**, *51E*, 2308.
- (14) Goyal, P. S.; Dasannacharya, B. A.; Kelkar, V. K.; Manohar, C.; Rao, K. S.; Valaulikar, B. S. *Physica B* **1991**, *174*, 196.
- (15) (a) Zaccai, G.; Blasie, J. K.; Schoenborn, B. P. *Proc. Natl. Acad. Sci. U.S.A.* **1975**, *72*, 376. (b) Andersen, H. C. *Annu. Rev. Biochem.* **1978**, *47*, 359.
- (16) Hirata, H.; Hattori, N.; Ishida, M.; Okabayashi, H.; Frusaka, M.; Zana, R. *J. Phys. Chem.* **1995**, *99*, 17778.
- (17) Shinitzky, M.; Barenholz, Y. *Biochim. Biophys. Acta* **1978**, *515*, 367.
- (18) (a) Hayter, J. B.; Penfold, J. *Colloid Polym. Sci.* **1983**, *261*, 1022. (b) Hayter, J. B.; Penfold, J. *Mol. Phys.* **1981**, *42*, 109. (c) Hansen, J.-P.; Hayter, J. B. *Mol. Phys.* **1982**, *46*, 109. (d) Hayter, J. B.; Penfold, J. *J. Chem. Soc., Faraday Trans. 1* **1981**, *77*, 1851.
- (19) (a) Chen, S. H. *Annu. Rev. Phys. Chem.* **1986**, *37*, 351. (b) Chen, S. H.; Lin, T. L. *Methods of Experimental Physics*; Academic Press: New York, 1987; Vol. 23B, p 489.
- (20) Danino, D.; Talmon, Y.; Zana, R. *Langmuir* **1995**, *11*, 1448.
- (21) Israelachvili, J. N.; Mitchell, D. J.; Ninham, B. *J. Chem. Soc., Faraday Trans. 2* **1976**, *72*, 1525.
- (22) Tanford, C. *J. Phys. Chem.* **1972**, *76*, 3020.
- (23) Alami, E.; Beinert, G.; Marie, P.; Zana, R. *Langmuir* **1993**, *9*, 1465.
- (24) Diamant, H.; Andelman, D. *Langmuir* **1994**, *10*, 2910.
- (25) Fuhrhop, J. H.; Fritsch, D. *Acc. Chem. Res.* **1986**, *19*, 130.
- (26) Zana, R. *J. Colloid Interface Sci.* **1980**, *78*, 330.
- (27) Blatt, F.; Ghiggino, K. P.; Sawyer, W. H. *J. Phys. Chem.* **1982**, *86*, 4461.
- (28) Shobha, J.; Balasubramanian, D. *Proc. Indian Acad. Sci. (Chem. Sci.)* **1987**, *98*, 469.

JP9535598